J. Braz. Chem. Soc., Vol. 18, No. 8, 1537-1546, 2007.
Printed in Brazil - ©2007 Sociedade Brasileira de Química
0103 - 5053 $6.00+0.00

Article

A Computational Study of Substituted Flavylium Salts and their Quinonoidal Conjugate-Bases: $S_0 \rightarrow S_1$ Electronic Transition, Absolute pK_a and Reduction Potential Calculations by DFT and Semiempirical Methods

Adilson A. Freitas,[a] K. Shimizu,[a] Luís G. Dias[b] and Frank H. Quina[,c]*

[a]*Instituto Superior Técnico, Universidade Técnica de Lisboa, Lisboa, Portugal*

[b]*Departamento de Química, Faculdade de Filosofia, Ciências e Letras de Ribeirão Preto, Universidade de São Paulo, 14040-901 Ribeirão Preto-SP, Brazil*

[c]*Instituto de Química, Universidade de São Paulo, 05513-970 São Paulo-SP, Brazil*

As transições eletrônicas para os cátions flavílio e bases quinonoidais de dezessete sais deste cátion foram estudadas nos níveis semiempírico e DFT (teoria do funcional da densidade). O efeito do solvente nos espectros eletrônicos foi incluído pelo Modelo Contínuo Polarizado, PCM. As transições eletrônicas de menor energia foram assinaladas como transições HOMO→LUMO. Ambos os níveis de teoria forneceram bons resultados para as transições eletrônicas dos cátions flavílio, enquanto apenas os cálculos por TDDFT-PCM puderam ser empregados para as transições das bases quinonoidais. Foram feitos cálculos de pK_a absoluto para nove sais de flavílio em nível DFT. Os valores de pK_a calculados pela nossa parametrização do PCM forneceram resultados excelentes, com um desvio médio absoluto de menos de meia unidade de pK_a. Foram calculados por DFT potenciais de redução para cinco cátions flavílio. Os resultados teóricos encontrados ficaram em boa concordância com os resultados experimentais após a correção de um desvio sistemático.

The electronic transitions for flavylium cations and quinonoidal bases of 17 substituted flavylium salts have been studied at semiempirical and DFT (density functional theory) levels. Solvent effect on electronic spectra was included by Polarizable Continuum Model, PCM. We assigned longest-wavelength absorption maxima to HOMO→LUMO transition. Both levels of theory gave good results for electronic transitions of flavylium cations whereas only TDDFT-PCM calculations could be used for electronic transitions of their quinonoidal bases. We also performed absolute pK_a calculations of nine flavylium salts at DFT level. The pK_a calculated values by our PCM parameterization gave excellent results with mean absolute deviation less than a half of one pK_a unit. One-electron reduction potentials were carried out for 5 flavylium cations at DFT level. The theoretical results found were in good agreement with experimental values after adjustment for a systematic deviation.

Keywords: flavylium salts, anthocyanins, quinonoidal base, pK_a calculation, time dependent-DFT

Introduction

Anthocyanins constitute the major red and purple pigments in plants and can be found in fruits, flowers and leaves.[1,2] Interest in the anthocyanins stems from the fact that they are omnipresent in our diet, exhibit unusual chemical and photochemical properties,[3-9] and have potential for application as food dyes[1] and antioxidant additives.[10,11] The basic chromophore of anthocyanins is the 7-hydroxyflavylium ion (Figure 1). In nature, the flavylium ion typically has hydroxyl substituents at positions 3 (always glycosylated) and 5 (occasionally glycosylated) and the phenyl or B-ring has one or more hydroxyl or methoxy substituents.[1] The colors of natural

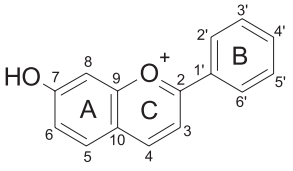

Figure 1. Planar structure and numbering of the 7-hydroxyflavylium ion.

*e-mail: quina@usp.br; frhquina@iq.usp.br

and synthetic anthocyanins range from yellow to purple, depending on the degree of substitution of the 7-hydroxyflavylium ion chromophore.

Rationalization of the chemical and photochemical properties of anthocyanins is complicated by the fact that, in aqueous solution, anthocyanins can exist in at least five different forms coupled via pH-dependent equilibria[7] (Scheme 1). At pH < 3, the dominant form is the flavylium cation (AH^+), which in fact is an excellent electron acceptor.[12-15] At physiological pH values, the dominant form of anthocyanins is typically the hemiacetal (B), in equilibrium with minor amounts of the isomeric chalcones (C_E and C_Z).[3] In the last few years, substantial progress has been made in understanding several aspects of the complex chemistry and photochemistry of anthocyanins. Many of the factors that affect the ground state equilibria of anthocyanins (Scheme 1) are much better understood and these equilibria (and hence anthocyanin color) can be manipulated in micellar media by appropriate choice of the detergent.[16,17] Methodology for studying the dynamics of proton transfer in the ground state in water and at micellar surfaces has been developed[17-20] and studies of anthocyanin-copigment complexes have demonstrated the importance of charge-transfer interactions in copigmentation.[21,22] Both natural anthocyanins and synthetic 7-hydroxyflavylium ions are superphotoacids in the lowest excited singlet state, undergoing ultrafast adiabatic excited-state proton transfer to water on the picosecond timescale.[19,20,23,24] These redox properties, as well as the pH-dependence and facile extraction from natural renewable sources, make anthocyanins interesting for applications in organoelectronic and photovoltaic devices.[25]

The complexity of the pH-dependent chemistry of anthocyanins makes it difficult to quantify experimentally many of the important properties of anthocyanins and of synthetic flavylium ions in aqueous solution. Thus, measurement of the acidity constant, pK_a, of the ground state of AH^+ often requires the use of fast reaction techniques[5] (stopped flow) due to the rapidity of the competitive hydration reaction of AH^+. The fact that hydration leads to the formation of the hemiacetal (B) and the isomeric chalcones (C_E and C_Z) complicates the determination of the electronic spectra of the quinonoidal base (A). Finally, in aqueous solution, the one-electron reduction of AH^+ is an electrochemically irreversible process,[21] resulting in large uncertainties in the redox potentials of anthocyanins. For these reasons, quantum chemical calculations of these properties are potentially of great utility for the comprehension of the complex ground and excited state reactivity of anthocyanins.

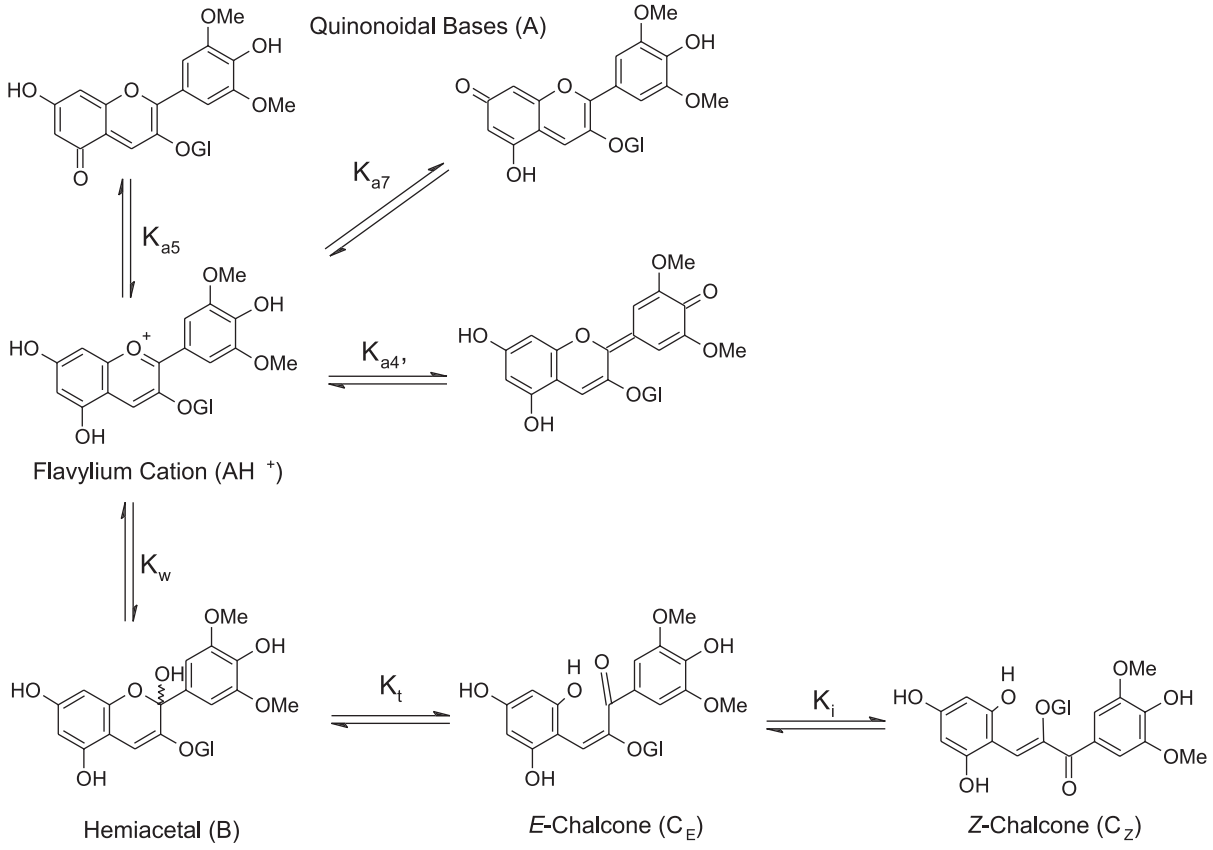

Scheme 1.

Rather surprisingly, however, relatively few theoretical studies of anthocyanins have been reported in the literature. Moreover, the majority of these have been at the semi-empirical level and have focused on the cationic form AH^+. These include calculations of: (a) the electronic transition energies of flavylium cations at the Huckel,[26] Pariser-Pople-Parr[27] or CNDO/2 level;[28] (b) the apparent equilibrium constant for the acid-base equilibrium, pK_{ap}, via molecular descriptors;[29,30] (c) the stability of the acid and base forms of anthocyanins based on the concepts of relative and absolute hardness;[31] (d) the geometry and internal rotational barriers of flavylium cations at both the semi-empirical and *ab initio* levels;[32-34] (e) the electronic spectra and solvatochromism of flavylium cations at the semi-empirical level;[35,36] and (f) the geometry and electronic transitions of the cation form of anthocyanins by density functional theory (DFT).[34,37]

In the present work, we present the results of a systematic quantum chemical study of the cationic form (AH^+) and the neutral quinonoidal base form (A) of a series of anthocyanins analogues at the *ab initio* level. The calculated properties include molecular geometries and electronic transition energies and oscillator strengths of AH^+ and A in the gas phase and in water and the pK_a values and one-electron reduction potentials of AH^+ in water. In general, the calculated values compare quite favorably with experimental values of these properties.

Computational Methodology

Building the initial geometries and optimization

The initial structures of the compounds were prepared with GaussView2.0 and Molden4.0.[38] The geometries were then fully optimized at B3LYP[39] and mPW1PW91[40] levels in vacuum using the 6-31+G(d,p) basis set and in implicit solvent using the 6-31G(d) basis set. The implicit solvent was described by the Integral Equation Formalism for the Polarizable Continuum Model,[41] IEFPCM, using the united atom topological model,[42] UA0, to build the molecular cavity.

The singlet transition energies and oscillator strengths

The vertical singlet electronic transition energies and oscillator strengths were computed by Time-Dependent DFT,[43] TDDFT, and TDDFT-PCM[44] at the mPW1PW91/6-31+G(d) and B3LYP/6-31+G(d) levels employing fully optimized geometries in implicit solvent model. Electronic transition calculations were also performed at the INDO-CIS[45] level on fully optimized geometries at the AM1[46] level in vacuum.

The absolute pK_a calculations

The thermodynamic cycle used for calculation of the absolute pK_a is shown in Scheme 2. The protonated flavylium or acid form, denoted AH^+, typically has a net charge of +1, while the corresponding quinonoidal base or deprotonated form, A, is typically neutral. The expressions utilized for the pK_a calculations are given below:

$$pK_a = \Delta G_{AH^+}(aq)/2.303RT \quad (1)$$

$$\Delta G_{AH^+}(aq) = \Delta G_{AH^+}(g) + \Delta\Delta G_{AH^+}(solv) \quad (2)$$

$$\Delta G_{AH^+}(g) = G_A(g) + G_{H^+}(g) - G_{AH^+}(g) \quad (3)$$

$$\Delta\Delta G_{AH^+}(solv) = \Delta G_A(solv) + \Delta G_{H^+}(solv) - \Delta G_{AH^+}(solv) \quad (4)$$

where $G_i(g)$ is the standard free energy of the molecular species "i" in gas phase, $\Delta G_i(solv)$ is the solvation free energy of "i" and $G_i(aq)$ is the free energy change for deprotonation in aqueous phase.

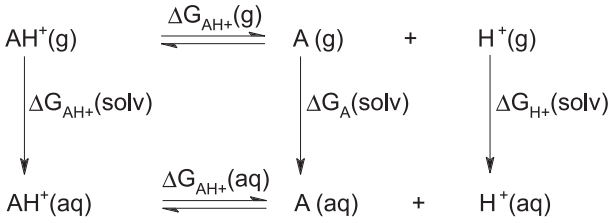

Scheme 2. The thermodynamic cycle employed for pK_a calculation.

The $G_{H+}(g)$ and $\Delta G_{H+}(solv)$ terms are –6.28 kcal/mol[47] and –263.98 kcal/mol,[48] respectively, and a term –RTln(24.46) was added to take into account the transformation of concentration units in the aqueous phase (atm to mol dm^{-3}).

The translational, rotational, and vibrational contributions to the gas phase free energy of the molecules were calculated within the framework of statistical thermodynamics.[49] Unscaled harmonic frequencies at the mPWIPW91/6-31+G(d,p) level were used in the vibrational contribution calculation. All stationary points were minima on the electronic energy hypersurface (only real numbers were found). Moreover, the electronic contribution to the gas phase free energy was obtained by single-point calculations with a 6-311+G(2d,2p) basis set and fully optimized structures.

The solvation free energies were calculated by IEFPCM at the mPW1PW91/6-31G(d)// mPW1PW91/6-31G(d) level with UA0 radii, by IEFPCM at the HF/6-31G(d)// mPW1PW91/6-31G(d) level with UAHF radii[50] and by

Solvation Model v5.4,[51] SM5.4, at the PM3//mPW1PW91/6-31G(d) level. All of the optimized geometries in solvent were obtained by IEFPCM at the mPW1PW91/6-31G(d) level with UA0 radii.

All geometry optimization and frequency calculations, TDDFT, INDO-CIS and IEFPCM were performed with the Gaussian03 package.[52] Calculations were performed on two PCs (PentiumIV and AMD) with the Linux operational system.

Reduction potential calculations for AH^+

The one-eletron reduction potentials of AH^+ were calculated through the thermodynamic cycle shown in Scheme 3. The reduced form of the flavylium cation, denoted $AH^{\cdot}$, is a neutral radical. The geometry optimisation and frequency calculations for this species were carried out using the unrestricted forms of the same functionals employed for the pK_a calculations. The solvation free energies were computed by IEFPCM at the UHF/6-31G(d)//UmPW1PW91/6-31G(d) level with UAHF radii. The expressions utilized for the one-eletron absolute reduction potential calculations are given below:

$$E^0 = -\frac{\Delta G^0_{AH^+}(aq)}{nF} \quad (5)$$

$$\Delta G^0_{AH^+}(aq) = \Delta G^0_{AH^+}(g) + \Delta\Delta G^0_{AH^+}(solv) \quad (6)$$

$$\Delta G^0_{AH^+}(g) = G^0_{AH^{\bullet}}(g) - G^0_{AH^+}(g) \quad (7)$$

$$\Delta\Delta G^0_{AH^+}(solv) = \Delta G^0_{AH^{\bullet}}(solv) - \Delta G^0_{AH^+}(solv) \quad (8)$$

Redox potentials are presented relative to a reference potential, in general relative to the normal hydrogen electrode (NHE). The absolute reduction potential of the NHE were calculated by using the same expressions presented above and experimental values tabulated in the NIST Chemistry Webbook[53] (ΔG^0_{H+} (solv) = 263.98 kcal mol^{-1}; $\Delta G^0_{H_2}(g)$ = 359.4 kcal mol^{-1};$\Delta G^0_{H_2}(g)$ = –9.32 kcal mol^{-1} and $\Delta G^0_{H_2}(g)$ = –1.4 kcal mol^{-1}). Experimental values for the NHE were employed to minimize possible errors from the calculation.

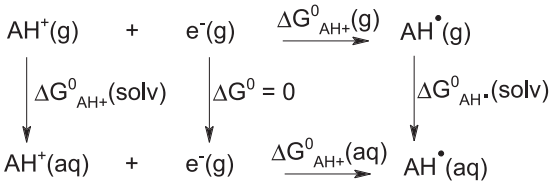

Scheme 3. The thermodynamic cycle employed for one-electron reduction potential calculation of flavylium cation.

Results and Discussion

Experimental data for the flavylium salts in aqueous solution were taken from the literature and are summarized in Table 1. Only flavylium salts for which data were available for electronic transitions of both the acid and base forms were included in this work.

All compounds in Table 1, except compound 18, have an OH group at C7 in the A ring and their corresponding quinonoidal conjugated-bases are produced by the deprotonation of this group.[17,63] In the case of the 4′-hydroxyflavylium ion (compound 18), the quinonoidal base must necessarily be formed by deprotonation of the OH group at C4′. In compound 14, the first deprotonation is of the COOH group at C4, followed by the OH group at higher pH (indicated as compound 15 in Table 1). Thus, this compound differs from other flavylium ions because deprotonation of OH group leads from a zwitterionic flavylium to an anionic quinonoidal base.

The bond lengths and internal angles of the flavylium cations and the quinonoidal bases in vacuum and in continuum solvent are practically the same for full optimization at either the B3LYP or mPW1PW91 levels (see Electronic Supplementary Information). Inspection of those data indicates that, on the average, the bond lengths r(O-C2) and r(C2-C1') are slightly longer at the AM1 (only gas phase) and B3LYP levels than at the mPW1PW91 level (gas or aqueous phase) for both the flavylium ion and the quinonoidal base. The average bond angle α(C9-O-C2) is larger at the DFT level than at the AM1 level in the gas phase, without significant alteration in the aqueous phase for either the flavylium ion or quinonoidal base. The average dihedral angle θ(O-C2-C1'-C6') points to coplanarity for flavylium cations at the AM1 and DFT levels in both the gas and aqueous phases, but a reasonable number of twisted quinonoidal bases may be found in the gas and aqueous phases at both levels of theory.

It is known, however, that flavylium salts can have twisted and perpendicular conformers in solution and that DFT methods overestimate the barrier to rotation of the dihedral angle θ(O-C2-C1'-C6') by at least 2 kcal mol^{-1} compared to many-body perturbation theory.[7] This torsional barrier overestimation by DFT methods must also be expected for quinonoidal bases.

The $S_0 \rightarrow S_1$ electronic transition

The electronic transitions of flavylium cations have been studied by semiempirical methodologies (e.g., PPP, CNDO, INDO) that included a truncated version of the

Table 1. Substituents of flavylium salts studied (see Figure 1), together with experimental pK_as and longest-wavelength absorption maxima of the acid and base forms. Except for 4´-hydroxyflavylium ion, compound 18, all of the other compounds have an OH group at C7 in the A ring

compd.	acid λ_{max} (nm)	base λ_{max} (nm)	pK_a	3	4	5	3'	4'	5'
1	530[a]	573[a]	-	OCH_3	H	OCH_3	OCH_3	OH	OCH_3
2	427[b]	475[c]	3.55[i]	H	H	H	H	H	H
3	467[b]	493[c]	-	H	H	H	OCH_3	OCH_3	H
4	457[b]	483[c]	-	H	H	H	H	OCH_3	H
5	468[b]	495[b]	-	H	H	H	OCH_3	OH	H
6	507[a]	559[a]	-	OCH_3	H	OCH_3	H	OH	H
7	456[d]	495[d]	4.00[d]	H	H	H	H	OH	H
8	462[e]	500[e]	-	H	H	OCH_3	H	OH	H
9	480[e]	498[e]	-	H	H	OH	OH	OCH_3	H
10	448[f]	480[f]	4.30[j]	H	CH_3	OH	H	OCH_3	H
11	468[e]	496[e]	4.20[j]	H	H	OH	H	OH	H
12	458[g]	492[g]	4.44[g]	H	Ph	H	H	OCH_3	H
13	417[d]	464[d]	4.40[d]	H	CH_3	H	H	H	H
14	484	460[c]	0.7[k]	H	COOH	H	H	OCH_3	H
15	-	494[c]	4.92[l]	H	COO^-	H	H	OCH_3	H
16	445[f]	475[f]	4.85[j]	H	CH_3	H	H	OCH_3	H
17	442[f]	475[f]	4.84[g]	H	CH_3	H	H	OH	H
18	436[h]	500[h]	4.61[l]	H	H	H	H	OH	H

[a] Ref. 54; [b] Ref. 55; [c] Ref. 56; [d] Ref. 18; [e] Ref 57; [f] Ref. 58; [g] Ref. 59; [h] Ref. 60; [i] Ref. 5; [j] Ref. 61; [k] Ref. 20; [l] Ref. 62

Table 2. Calculated oscillator strengths, f, percent contribution of HOMO→LUMO excitation, %H→L, and longest-wavelength absorption maxima, λ_{max}, of flavylium cations

compd.	AM1/ZINDO			TDDFT-PCM (B3LYP)			TDDFT-PCM (mPW1PW91)		
	f	%H→L	λ_{max}	f	%H→L	λ_{max}	f	%H→L	λ_{max}
1	0.858	87.1	511	0.627	77.5	484	0.642	76.8	485
2	0.809	94.3	447	0.654	80.7	407	0.683	82.4	394
3	0.946	90.5	476	0.506	82.2	483	0.929	83.0	421
4	0.948	93.1	471	0.930	81.6	430	0.929	82.9	415
5	0.906	87.7	471	0.510	81.1	476	0.897	82.4	425
6	0.862	93.5	504	0.535	74.9	487	0.582	77.4	470
7	0.924	93.4	469	0.884	81.0	428	0.914	82.4	414
8	0.928	92.3	472	0.609	71.5	445	0.670	74.8	429
9	0.931	86.6	475	0.625	77.6	466	0.676	78.2	447
10	0.923	90.5	453	0.530	69.5	435	0.589	73.0	419
11	0.933	92.4	470	0.538	67.6	444	0.602	71.5	428
12	0.745	91.2	458	0.875	83.0	442	0.638	83.3	424
13	0.759	93.5	430	0.610	81.6	405	0.626	83.1	390
14	0.908	93.1	507	0.758	79.9	481	0.803	81.4	459
16	0.908	91.9	455	0.906	82.2	426	0.936	83.5	411
17	0.883	92.3	452	0.862	81.6	424	0.893	82.9	410
18	0.915	92.9	476	0.859	81.1	435	0.892	82.5	419

full configuration interaction (typically, only single excitation determinants were taken into account).[29,37,64,65] In this work, INDO-CIS and TDDFT methodologies were used in electronic excitation calculations on flavylium cations and their quinonoidal conjugate-bases. In addition, solvent effects on absorption spectra were incorporated by TDDFT-PCM single-point calculations on fully optimized geometries in the aqueous phase.

The results are summarized in Figures 2 and 3 and Tables 2 and 3. Table 2 shows the longest wavelength absorption band of the substituted flavylium cations. Some trends may be noted: *i*) the experimental data, listed in Table 1, are distributed rather uniformly over the range from 415 to 530nm; *ii*) while TDDFT systematically underestimates the wavelengths, INDO-CIS with fully optimized geometries at the AM1 level (the methodology with lowest computational cost) provides results in much better agreement with experiment; *iii*) comparison between TDDFT and TDDFT-PCM at the mPW1PW91 /6-31+G(d) level points to only a small effect of continuum-dielectric solvent. The same trend is obtained at the B3LYP level (results not shown); *iv*) TDDFT-PCM calculations at the B3LYP/6-31+G(d) level are closer to experiment

than those at the mPW1PW91/6-31+G(d) level. However, calculations at the mPW1PW91/6-31+G(d) level exhibit less spread within the data range.

For all flavylium ions, the transition from the ground state to the first excited state is predominantly a HOMO→LUMO transition, where the HOMO and LUMO are π and π* molecular orbitals, respectively. The oscillator strengths, with percent contribution of the HOMO→LUMO configuration, are given in Table 2. This percent contribution is calculated by taking into account the intermediate normalization of the CIS expansion (*i.e.*, the summation of the squares of the CIS-coefficients is equal to 0.5).

Table 3 summarizes the result for quinonoidal bases. The following trends may be noted: *i*) the experimental data, listed in Table 1, are concentrated between 490 and 500nm; *ii*) the AM1/INDO-CIS calculations are not useful: the predicted excitations all lie around 450 nm (the exception is compound 14); *iii*) inclusion of the solvent effect, treated as a continuum-dielectric medium, leads to less disperse numbers that are closer to the experimental values. The comparison was done at the mPW1PW91/6-31+G(d) level, but is also valid at the B3LYP/6-31+G(d) level (results not shown); *iv*) as for flavylium cations, the TDDFT-PCM calculations at the B3LYP/6-31+G(d) level are a little better than at the mPW1PW91/6-31+G(d) level.

For the quinonoidal bases, the electronic transition from S_0 to S_1 is also dominated by the HOMO→LUMO configuration. Table 3 shows the oscillator strengths and percent contribution of the HOMO→LUMO configuration. Overall, the oscillator strengths are lower for the TDDFT-PCM methodologies than from INDO-CIS calculations. Furthermore, INDO-CIS suggests a higher contribution from the HOMO→LUMO configuration in the $S_0 \rightarrow S_1$ transition.

The TDDFT-PCM calculations exhibit a net shift relative to the experimental data. This effect has been reported in the literature.[66-68] Parac and Grimme analyzed the accuracy of TDDFT methods for predicting the π→π* transition in polycyclic aromatic molecules.[66] They found different trends (*i.e.*, overestimated or underestimated excitation energies) depending on the functional employed and its performance in the description of polar or ionic excited states. They also suggested that the development of new functionals should concentrate not only on the asymptotic behavior of the exchange-correlation potential, but also on the description of intermediate regions. Here, a uniform offset is used to correct the TDDFT-PCM calculations for both the acid and base forms.[67,68] The offset depends on the functional and the corrected predictions are shown in Figures 2 and 3. After the offset, the TDDFT-PCM calculations at the mPW1PW91/6-31+G(d) level are in slightly better agreement with the experimental data than those at B3LYP level.

It has been proposed that non-planar conformers of flavylium salts play an important role in determining the fluorescence quantum yield due to relaxation to a twisted intramolecular charge transfer (TICT) state.[36] Hence, some exploratory calculations were performed to gain information about the possible contribution of

Table 3. Calculated oscillator strengths, f, percent contribution of HOMO→LUMO excitation, %H→L, and longest-wavelength absorption maxima, λ_{max}, of quinonoidal bases

compd.	AM1/ZINDO			TDDFT-PCM (B3LYP)			TDDFT-PCM (mPW1PW91)		
	f	%H→L	λ_{max}	f	%H→L	λ_{max}	f	%H→L	λ_{max}
1	0.724	92.7	459	0.534	75.6	524	0.554	77.0	509
2	0.764	93.4	447	0.489	78.1	457	0.511	79.6	442
3	0.817	93.7	451	0.694	80.0	474	0.683	80.3	452
4	0.818	93.9	452	0.661	78.9	464	0.684	80.3	450
5	0.805	93.4	450	0.642	78.7	466	0.665	80.2	451
6	0.724	93.4	460	0.510	75.6	517	0.530	77.2	502
7	0.808	93.8	451	0.641	78.7	464	0.652	79.7	451
8	0.771	93.1	449	0.547	77.9	469	0.552	79.4	453
9	0.771	92.8	447	0.570	77.7	476	0.589	78.9	459
10	0.725	92.7	450	0.483	78.8	467	0.507	80.2	451
11	0.772	93.1	450	0.525	77.0	469	0.546	71.5	452
12	0.745	93.5	456	0.544	79.3	478	0.568	81.0	461
13	0.720	94.0	448	0.431	79.1	466	0.453	80.6	451
14	0.029	0	476	0.777	81.4	435	0.803	82.4	419
15	0.360	50.0	454	0.555	78.9	471	0.578	80.3	455
16	0.765	93.9	453	0.584	79.6	470	0.607	81.1	453
17	0.757	93.9	455	0.567	79.4	475	0.590	81.0	459
18	1.287	94.6	457	0.930	73.5	447	0.977	75.5	434

non-planar conformations to the absorption spectra. It was observed that conformations of ± 30° around the optimized structure only slightly change the electronic transitions for flavylium cations and quinonoidal bases. Reducing the degree of coplanarity to the fully orthogonal conformation shifts the maxima to shorter wavelengths by ca. 40 nm. Furthermore, the oscillator strength was reduced by half. Based on these results we can conclude that the use of the optimized near-planar structure is adequate to describe the absorption spectra properly.

The absolute pK_a calculation

The literature concerning pK_a prediction for flavylium salts is scarce and based on quantitative structure-property relationship, QSPR, models using molecular or topological descriptors.[29,30] Absolute pK_a calculation by theoretical methods is feasible after the definition of a convenient thermodynamic cycle (Scheme 2). The major problem is how to achieve chemically useful accuracy: an error of 1.36 kcal mol^{-1} in $\Delta G_{AH+}(aq)$ (equation 1) results in an error of ± 1 pK_a unit.[69] Fortunately, the recent work of Shields and co-workers[70] has shown that absolute pK_a values for a set of carboxylic acids and phenols can be predicted to within ± 0.5 pK_a unit. They have used state-of-the-art calculations for accurate thermochemistry in the gas phase via Gaussian-*n*[71] and CBS[72] methods combined with the conductor polarizable continuum model,[73] CPCM.

Absolute pK_as were obtained following the ideas outlined in recent work of Saracino et al.[74] The procedure is detailed in the computational methodology. Table 4 summarizes the numerical results for the different methodologies used in the pK_a calculations. All the methodologies employed fully optimized geometries and frequencies at the mPW1PW91/6-31+G(d,p) level in the gas phase with single-point calculations at the mPW1PW91/6-311+G(2d,2p) level. In addition, the geometries in the solvent were fully optimized at the mPW1PW91/6-31G(d) level by IEFPCM with UA0 radii.

Four different approaches were used to estimate the hydration free energies: *i*) Approach 1 used single point calculations at the HF/6-31G(d) level and IEFPCM with UAHF radii; *ii*) Approach 2, employed single point calculations at the mPW1PW91/6-31G(d) level and IEFPCM with UA0 radii; *iii*) Approach 3, consisted of single point calculations at the PM3 level and SM5.4; *iv*) Approach 4 used single point calculations at the HF/6-31G(d) level and our PCM parameterization[75] with Bondi atomic radii[76].

Clearly, Approach 2 is useless for prediction of absolute pK_as. The calculated values are in the range of 6.5 and 8.5, while the experimental data range from 3.5 to 5.5. This is not unexpected since the recommended approach for good predictions of hydration free energies in PCM is Approach 1.[77] Although Approach 1 produced better results than Approach 2, the predicted values are still not satisfactory. Only Approaches 3 and 4 can be considered to be useful for predicting absolute pK_as to within ± 1 pK_a unit. Closer inspection of Table 4 shows that Approach 3 has many outliers and that Approach 4 is the only one leading to values within ± 0.5 pK_a unit.

Reduction potentials of AH^+

The difficulty of obtaining experimentally reliable redox potentials for AH^+ is reflected in the small number of literature values listed in Table 5. The solvation free energy calculations were carried out only at the UHF level because the SM5.4 model implemented in AMSOL does not support open shell calculations and our PCM parameterization was not optimized for open shell structures. The results show a systematic deviation in comparison to experimental values. The energies calculated with spin-unrestricted wavefunctions for flavylium cations gave exactly the same values obtained from closed shell calculations, indicating that the

Table 4. The experimental (from Table 1) and calculated pK_as by approaches 1, 2, 3 and 4 (at 298.15K, 1 atm). The bottom row shows the mean absolute deviation, MAD, between the experimental data and the theoretical approach

compd.	pK_a (exp)	pK_a^1	pK_a^2	pK_a^3	pK_a^4
2	3.55	4.04	6.75	3.44	3.82
7	4.00	5.11	7.26	4.61	4.17
10	4.30	6.54	8.46	6.65	5.46
11	4.20	5.95	7.39	4.97	4.22
12	4.44	4.38	6.58	4.54	3.88
13	4.40	4.99	7.38	4.45	4.32
16	4.85	6.48	7.63	5.60	5.04
17	4.84	6.47	7.88	5.31	4.72
18	4.61	5.35	8.01	4.80	4.99
MAD		1.14	3.13	0.60	0.33

Table 5. Experimental and calculated one-electron reduction potentials (E) for flavylium cations, in Volts. The tabulated potentials are referenced to the normal hydrogen electrode (NHE), at T = 298.15K

flavylium cation (compd.)	E_{exp}	E_{calc}	$E_{corr}(E_{calc} + 0,41)$
4'-hydroxyflavylium (**18**)	0.056[a]	-0.339	0.066
3,7,4'-trihydroxyflavylium	-0.059[b]	-0.490	-0.085
7-methoxy-4-methylflavylium	-0.079[c]	-0.454	-0.049
7,4'-dihydroxyflavylium (**7**)	-0.084[d]	-0.513	-0.101
3,5,7,4'-tetrahydroxyflavylium	-0.164[e]	-0.541	-0.136

[a] Ref. 14; [b] Ref. 12; [c] Ref. 21; [d] Ref. 13; [e] Ref 15.

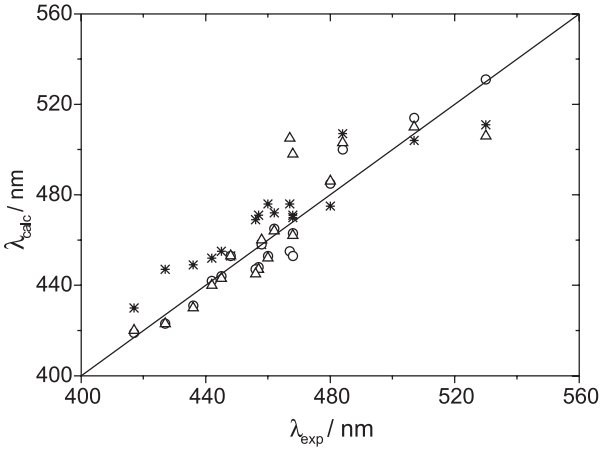

Figure 2. Calculated excitation energies for flavylium cations. *Stars* denote INDO-CIS single-point calculations on fully optimized AM1 geometries; *triangles* denote TDDFT-PCM single-point calculations at the B3LYP/6-31+G(d) level on fully optimized geometries at the B3LYP/6-31G(d) level using PCM(UA0); *circles* denote TDDFT-PCM single-point calculations at the mPW1PW91/6-31+G(d) level on fully optimized geometries at the mPW1PW91/6-31G(d) level using PCM(UA0). Excitation energies at the B3LYP and mPW1PW91 levels were shifted downwards by 0.11 eV and 0.22 eV, respectively. The solid line is $\lambda_{calc} = \lambda_{exp}$.

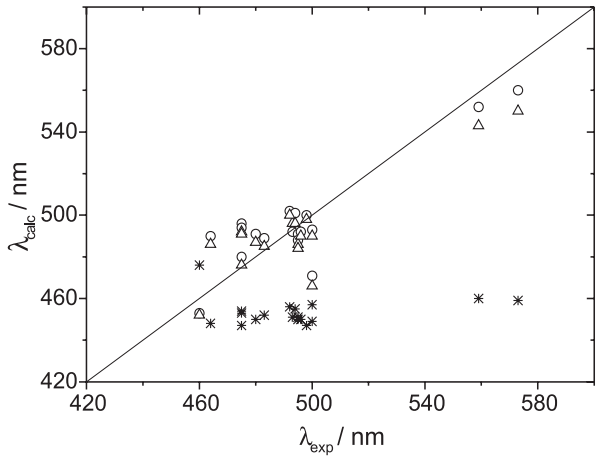

Figure 3. Calculated excitation energies for quinonoidal bases. Symbols as in Figure 3. Excitation energies at the B3LYP and mPW1PW91 levels were shifted downwards by 0.11 eV and 0.22 eV, respectively. The solid line is $\lambda_{calc} = \lambda_{exp}$.

additional degree of freedom in open shell vs. closed shell calculations did not affect the results.

The deviation observed between experimental and calculated reduction potencials is attributed to the tendency of DFT to overstabilise delocalized p-systems. This behavior has been observed by other authors in analogous studies.[78,79] Summation of 0.41 V to the calculated reduction potentials gives corrected values that are in good agreement with the experimental ones. These results indicate that the metodology should be suitable for predicting redox potentials of flavylium cations.

Conclusions

Computational calculations with a practical level of theory presented in this work permit insight into the properties of flavylium cations and quinonoidal bases, the two colored species of anthocyanins. The longest absorption wavelength of flavylium cations can be adequately estimated by semiempirical methods, but the results for quinonoidal bases are quite unsatisfactory. TDDFT-PCM calculations employing fully optimized geometries in implicit solvent showed that the lowest energy transition is essentially a HOMO-LUMO transition, giving accurate results of λ_{max} for cations and, to a lesser extent, for quinonoidal bases. The TDDFT-B3LYP and TDDFT-mPW1PW91 calculations systematically overestimate the electronic transition energies of both species, easily corrected by shifting the energy downwards by 0.11 eV and 0.22 eV for B3LYP and mPW1PW91, respectively. The corrected results the for mPW1PW91 functional are in better agreement with experimental data.

Application of our recent parameterization of PCM to absolute pK_a calculations of flavylium salts showed excellent results. Moreover, the accuracy achieved of less than half of one pK_a unit is comparable to most refined and time demanding methods, the application of which to flavylium salts would be prohibitive due to the size of these compounds. After adjustment for a systematic deviation, calculated absolute reduction potentials also agree satisfactorily with experimental values. These results point to the possibility of theoretical design of new flavylium salts with specific properties.

Acknowledgments

This work was funded in part by a CAPES/GRICES (Brazil/Portugal) international cooperation grant, the CNPq (Universal 475337/2004-2) and in part by the National Science Foundation under grant MCB0315502. A. A. Freitas and K. Shimizu were FAPESP graduate fellows in Brazil (project numbers 01/00973-1 and 01/05852-8, respectively).

Supplementary Information

All optimized structures in Protein Data Bank, PDB, format, along with tables of selected structural parameters, including: bond length between C2 and the adjacent O atom in the C ring, r(O-C2); the bond length between carbons C2 and C1', r(C2-C1'); angle between the bonds

from oxygen to carbons C9 and C2, a(C9-O-C2); and dihedral angle defined by O, C2, C1' and C6', q(O-C2-C1'-C6'. Supplementary data are available free of charge at http://jbcs.sbq.org.br/ as PDF file.

References

1. Brouillard, R. In *Anthocyanins as Food Colours*; Markakis, P., ed.; Academic Press: New York, 1982, ch. 9.
2. Harborne, J. B.; Williams, C. A.; *Phytochemistry* **2000**, *55*, 481.
3. Brouillard, R.; Dubois, J. E.; *J. Am. Chem. Soc.* **1977**, *99*, 1359.
4. Brouillard, R.; Delaporte R.; *J. Am. Chem. Soc.* **1977**, *99*, 8461.
5. McClelland, R. A.; Gedge, S. J.; *J. Am. Chem. Soc.* **1980**, *102*, 5838.
6. Santos, H.; Turner, D. L.; Lima, J. C.; Figueiredo, P.; Pina, F.; Maçanita, A. L.; *Phytochemistry* **1993**, *33*, 1227.
7. Houbiers, C.; Lima, J. C.; Maçanita, A. L.; Santos, H.; *J. Phys. Chem. B* **1998**, *102*, 3578.
8. Lima, J. C.; Abreu, I.; Brouillard, R.; Maçanita, A. L.; *Chem. Phys. Lett.* **1998**, *298*, 189.
9. Figueiredo, P.; Lima, J. C.; Santos, H.; Wigand, M.-C.; Brouillard, R.; Pina, F.; Maçanita, A. L.; *J. Am. Chem. Soc.* **1994**, *116*, 1249.
10. Wang, H.; Cao, G.; Prior, R. L.; *J. Agric. Food Chem.* **1997**, *45*, 304.
11. Satué-Gracia, M. T.; Heinonen, M.; Frankel, E. N.; *J. Agric. Food Chem.* **1997**, *45*, 304.
12. Harper, K. A.; *Aust. J. Chem.* **1967**, *20*, 691.
13. Harper, K. A.; Chandler, B. V.; *Aust. J. Chem.* **1967**, *20*, 731.
14. Harper, K. A.; Chandler, B. V.; *Aust. J. Chem.* **1967**, *20*, 745.
15. Harper, K. A.; *Aust. J. Chem.* **1968**, *21*, 221.
16. Vautier-Giongo, C.; Yihwa, C.; Moreira Junior, P. F.; Lima, J. C.; Freitas, A. A.; Alves, M.; Quina, F. H.; Maçanita, A. L.; *Langmuir* **2002**, *18*, 10109.
17. Lima, J. C.; Vautier-Giongo, C.; Melo, E.; Lopes, A., Quina, F. H.; Maçanita, A. L.; *J. Phys. Chem. A* **2002**, *106*, 5851.
18. Maçanita, A. L.; Moreira Jr, P. F.; Lima, J. C.; Quina, F. H.; Yihwa, C.; Vautier-Giongo, C.; *J. Phys. Chem. A* **2002**, *106*, 1248.
19. Moreira Jr., P. F.; Giestas, L.; Yihwa, C.; Vautier-Giongo, C.; Quina, F. H.; Maçanita, A. L.; Lima, J. C.; *J. Phys. Chem. A* **2003**, *107*, 4203.
20. Paulo, L.; Freitas, A. A.; Silva, P. F.; Shimizu, K.; Quina, F. H.; Maçanita, A. L.; *J. Phys. Chem. A* **2006**, *110*, 2089.
21. Ferreira da Silva, P.; Lima, J. C.; Quina, F. H.; Maçanita, A. L.; *J. Phys. Chem. A* **2004**, *107*, 3263.
22. Ferreira da Silva, P.; Lima, J. C.; Freitas, A. A; Shimizu, K.; Quina, F. H.; Maçanita, A. L.; *J. Phys. Chem. A* **2005**, *109*, 7329.
23. Giestas, L.; Yihwa, C.; Lima, J. C.; Vautier-Giongo, C.; Lopes, A.; Quina, F. H.; Maçanita, A. L.; *J. Phys. Chem. A* **2003**, *107*, 3263.
24. Rodrigues, R.; Vautier-Giongo, C.; Silva, P. F.; Fernandes, A. C.; Cruz, R.; Maçanita, A. L.; Quina, F. H.; *Langmuir* **2006**, *22*, 933.
25. Cherepy, N. J.; Smestad, G. P.; Grätzel, M.; Zhang, J. Z.; *J. Phys. Chem. B*, **1997**, *101*, 9342.
26. Boyd, G. V.; Singer, N.; *Tetrahedron* **1965**, *21*, 1263.
27. Bendz, G.; Martensson, O.; Nilsson, E.; *Arkiv För Kemi* **1967**, *27*, 65; Kurtin, W. E.; Song, P. S.; *Tetrahedron* **1967**, *24*, 2255; Nilsson, E.; *Arkiv För Kemi* **1969**, *31*, 111; Singer, N.; Whittington, P. R.; Boyd, G. V.; *Tetrahedron* **1970**, *26*, 3731.
28. Martensson, O.; Warren, C. H.; *Acta Chem. Scand.* **1970**, *24*, 2745.
29. Amic, D.; Amic, D. D.; Bešlo, D.; Lucic, B.; Trinajstic, N.; *J. Chem. Inf. Comput. Sci.* **1999**, *39*, 967.
30. Peruzzo, P. J.; Marino, D. J. G.; Castro. E. A.; Toropov, A. A.; *J. Mol. Struct.* (*THEOCHEM*) **2001**, *572*, 53.
31. Amic, D.; Trinajstic, N.; *J. Chem. Soc. Perkin Trans. 2* **1991**, *6*, 891.
32. Pereira, G. K.; Donate, P. M.; Galembeck, S. E.; *J. Mol. Struct.* (*THEOCHEM*) **1996**, *363*, 87.
33. Pereira, G. K.; Donate, P. M.; Galembeck, S. E.; *J. Mol. Struct.* (*THEOCHEM*) **1997**, *392*, 169.
34. Meyer, M.; *Int. J. Quantum Chem.* **2000**, *76*, 724.
35. Pereira, G. K.; Galembeck, S. E.; *Spectrochim. Acta A* **1998**, *54*, 339.
36. Roshal, A. D.; Minayev, D. Yu.; Pedash, Yu. F.; Novikov, A. I.; *Polish J. Chem.* **2002**, *76*, 1301.
37. Woodford, J. N.; *Chem. Phys. Lett.* **2005**, *410*, 182.
38. Schaftenaar, G.; Noordik, J. H.; *J. Comput.-Aided Mol. Design* **2000** *14*, 123.
39. Becke, A. D.; *J. Chem. Phys.* **1993**, *98*, 5648.
40. Adamamo, C.; Barone, V.; *J. Chem. Phys.* **1998**, *108*, 664.
41. Mennucci, B.; Cammi, R.; Tomasi, J.; *J. Chem. Phys.* **1998**, *109*, 2798.
42. Rappe, A. K.; Casewit, C. J.; Colwell, K. S.; Goddard III, W. A.; Skiff, W. M.; *J. Am. Chem. Soc.* **1992**, *114*, 10024.
43. Stratmann, R. E.; Scuseria, G. E.; Frish, M. J.; *J. Chem. Phys.* **1998**, *109*, 8218.
44. Cossi, M.; Barone, V.; *J. Chem. Phys.* **2001**, *115*, 4708.
45. Zerner, M. C.; Loew, G. H.; Kirchner, R. F.; Westerhoff, U. T. M.; *J. Am. Chem. Soc.* **1980**, *102*, 589.
46. Dewar, M. J. S.; Zoebisch, E. G.; Healy, E. F.; Stewart, J. J. P.; *J. Am. Chem. Soc.* **1985**, *107*, 3902.
47. Topol, I. A.; Tawa, G. J.; Burt, S. K.; Rashin, A. A.; *J. Chem. Phys.* **1999**, *111*, 10998.
48. Tissandier, M. D.; Cowen, K. A.; Feng, W. Y.; Gundluach, E.; Cohen, M. H.; Earhart, A. D.; Coe, J. V.; Tutte, T. R.; *J. Phys. Chem. A* **1998**, *102*, 7787.

49. Hill, T. L. *An Introduction To Statistical Thermodynamics*; Addison-Wesley: Massachusetts, 1960.
50. Barone, V.; Cossi, M.; Tomasi, J.; *J. Chem. Phys.* **1997**, *107*, 3210.
51. Hawkins, G. D.; Giesen, D. J.; Lynch, G. C.; Chambers, C. C.; Rossi, I.; Storer, J. W.; Li, J.; Winget, P.; Rinaldi, D.; Liotard, D. A.; Cramer, C. J.; Truhlar, D. G.; *AMSOL-version 6.6*, 1999.
52. Frisch, M. J.; Trucks, G. W.; Schlegel, H. B.; Scuseria, G. E.; Robb, M. A.; Cheeseman, J. A.; Montgomery, J. A.; Vreven, T.; Kudin, K. N.; Burant, J. C.; Millam, J. M.; Iyengar, S. S.; Tomasi, J.; Barone, V.; Mennucci, B.; Cossi, M.; Scalmani, G.; Rega, N.; Peterson, G. A.; Nakatsuji, H.; Hada, M.; Ehara, M.; Toyota, K.; Fukuda, R.; Hasegawa, J.; Ishida, M.; Nakajima, T.; Honda, Y.; Kitao, O.; Nakai, H.; Klene, M.; Li, X.; Know, J. E.; Hratchian, H. P.; Cross, J. B.; Adamo, C.; Jaramillo, J.; Gomperts, R.; Stratmann, R. E.; Yazyev, O.; Austin, A. J.; Cammi, R.; Pomelli, C.; Ochterski, J. W.; Ayala, P. Y.; Morokuma, K.; Voth, G. A.; Salvador, P.; Dannenberg, J. J.; Zakrzewski, V. G.; Dapprich, S.; Daniels, A. D.; Strain, M. C.; Farkas, O.; Malick, D. K.; Rabuck, A. D.; Raghavachari, K.; Foresman, J. B.; Ortiz, J. V.; Cui, Q.; Baboul, A. G.; Clifford, S.; Cioslowski, J.; Stefanov, B. B.; Liu, G.; Liashenko, A.; Piskorz, P.; Komaromi, I.; Martin, R. L.; Fox, D. J.; Keith, T.; Al-Laham, M. A.; Peng, C. Y.; Nanayakkara, A.; Challacombe, M.; Gill, P. M. W.; Johnson, B.; Chen, W.; Wong, M. W.; Gonzalez, C.; Pople, J. A. *Gaussian 03, Revision B.04*, Gaussian, Inc., Pittsburgh PA, 2003.
53. U.S. Secretary of Commerce; *NIST Chemistry Webbook*, *Referência padrão - NIST n° 69,* http://webbook.nist.gov (accessed in March 2005).
54. Abe, K.; Sakaino, Y.; Kakinuma, J.; Kakisawa, H.; *Nippon Kagaku Kaishi* **1977**, *8*, 1197.
55. Jurd, L.; *J. Org. Chem.* **1963**, *28*, 987.
56. Jurd, L; Geissman, T. A.; *J. Org. Chem.* **1963**, *28*, 2394.
57. Baranac, J. M.; Amic, D. S.; *J. Agric. Food Chem.* **1990**, *38*, 2111.
58. Sweeny, J. G.; Iacobucci, G. A.; *J. Agric. Food Chem.* **1983**, *31*, 531.
59. Baranac, J.; Amic, D.; Vukadinovic, V.; *J. Agric. Food Chem.* **1990**, *38*, 932.
60. McClelland, R. A.; McGall, G. H.; *J. Org. Chem.* **1982**, *47*, 3730.
61. Brouillard, R.; Iacobucci, G. A.; Sweeny, J. G.; *J. Am. Chem. Soc.* **1982**, *104*, 7585.
62. Mazza, G.; Brouillard, R.; *J. Agric. Food Chem.* **1987**, *35*, 422.
63. Costantino, L.; Rastelli, G.; Rossi, M. C.; Albasini, A.; *J. Chem. Soc. Perkin Trans. 2*, **1995**, *2*, 227.
64. Torskangerpoll, K.; Børve, K. J.; Andersen, Ø. M.; Sæthre, L. J.; S*pectrochim. Acta A* **1999**, *55*, 761.
65. Lietz, H.; Haucke, G.; Czerney, P.; John, B.; *J. Prakt. Chem.* **1996**, *338*, 725.
66. Parac, M.; Grimme, S.; *Chem. Phys.* **2003**, *292*, 11.
67. Bauernschmitt, R.; Ahlrichs, R.; *Chem. Phys. Lett.* **1996**, *256*, 454.
68. Jacquemin, D.; Preat, J.; Charlot, M.; Wathelet, V.; André, J. M.; Perpète, E. A.; *J. Chem. Phys.* **2004**, *121*, 1736.
69. Liptak, M. D.; Shields, G. C.; *Int. J. Quantum Chem.* **2001**, *85*, 727.
70. Toth, A. M.; Liptak, M. D.; Phillips, D. L.; Shields, G. C.; *J. Chem. Phys.* **2001**, *114*, 4595.
71. Curtiss, L. A.; Raghavachari, K; Redfern, P. C.; Rassolov, V.; Pople, J. A. *J. Chem. Phys.* **1998**, *109*, 7764; Curtiss, L. A.; Raghavachari, K; Trucks, G. W.; Pople, J. A.; *J. Chem. Phys.* **1991**, *94*, 7221.
72. Montgomery, J. A.; Frisch, M. J.; Ochterski, J. W.; Petersson, G. A.; *J. Chem. Phys.* **1999**, *110*, 2822; Ochterski, J. W.; Petersson, G. A.; Montgomery, J. A.; *J. Chem. Phys.* **1996**, *104*, 2598; Petersson, G. A.; Malick, D. K.; Wilson, W. G.; Ochterski, J. W.; Montgomery, J. A.; Frisch, M. J.; *J. Chem. Phys.* **1998**, *109*, 10570.
73. Barone, V.; Cossi, M.; *J. Phys. Chem. A* **1998**, *102*, 1995.
74. Saracino, G. A. A.; Improta, R.; Barone, V.; *Chem. Phys. Lett.* **2003**, *373*, 411.
75. Shimizu, K.; Freitas, A. A; Farah, J. P. S.; Dias, L. G.; *J. Phys. Chem. A* **2005**, *109*, 11322.
76. Bondi, A.; *J. Phys. Chem.* **1964**, *68*, 441.
77. Zacharias, M.; *J. Phys. Chem. A* **2003**, *107*, 3000.
78. Lewis, A.; Bumpus, J. A.; Truhlar, D. G.; Cramer, C. J.; *J. Chem. Educ.* **2004**, *81*, 596.
79. Patterson, E. V.; Cramer, C. J.; Truhlar, D. G.; *J. Am. Chem. Soc.* **2001**, *123*, 2025.

Received: June 6, 2006
Web Release Date: December 11, 2007

FAPESP helped in meeting the publication costs of this article.